BEAM DUCTILITY EXPERIMENT USING GRADE 500 STEEL

Munaz A. Noor[1], FIEB, MASCE, MACI

ABSTRACT

The results of an experimental program on simply supported beams subjected to two point loading are presented. Nine specimens, with three different reinforcement ratio (equal to $\rho = 0.007, 0.009$ and 0.0128) and three different concrete strengths (equal to $f_c^{'} = 5.25$ ksi, 6.5 ksi and 7.25 ksi) have been tested. An attempt is made to classify the performance of the specimens according to the ductility they exhibited varying tensile steel ratio and concrete compressive strength. Moment-curvature relation, depth of neutral axis, strain in the materials are considered as performance criteria in this study.

Keywords: Beams, Ductility ratio, Grade 500, Reinforced Concrete

INTRODUCTION

There is a growing focus on the ductility of reinforcing steels following the introduction of Grade 500 steel in the Bangladesh Standard, BDS ISO 6935-2. This focus is driven primarily by relief of congestion; particularly in buildings assigned a high seismic design category. There are also other areas where high strength steel bar can help improve construction efficiencies, or - combined with high strength concrete - allow reinforced concrete to be used in more demanding applications. Actually, higher grades are often used to permit smaller concrete members, relating to the space problems for placement of the reinforcement. Even though the steel ordinarily constitutes only a few percent of the total volume of reinforced concrete, it is a major cost factor. This reduction in concrete member and percentage of steel tend to reduce the flexure stiffness and ductility of a member.

Flexural strength and stiffness can be easily evaluated using the ordinary beam bending theory, but there exists no simple method for evaluating the flexural ductility of an reinforced concrete (RC) beam. To evaluate the flexural ductility, it is necessary to conduct non-linear moment-curvature experiment or numerical

[1]Professor, Dept. of Civil Engineering., Bangladesh University of Engineering and Technology (BUET), Dhaka 1000. E-mail: mnoor@ce.buet.ac.bd

analysis, extended well into the post-peak range, of the beam section. Because of the difficulties involved, there have been few studies on the post-peak behaviour and flexural ductility of reinforced concrete members. From the structural safety point of view, ductility is as important as strength. Possession of good flexural ductility would enable a structure to dissipate excessive energy through inelastic deformations within the potential plastic hinge regions while maintaining sufficient flexural strength to resist applied loads. A relatively high level of flexural ductility would provide the structure an increased chance of survival against accidental impact and seismic attack. Flexural ductility is particularly important when the capacity design philosophy for seismic resistant structures is adopted.

According to this philosophy, which is also called the "strong column-weak beam" approach, the beams should yield before the columns yield and the beams should be required to have sufficient flexural ductility such that the potential plastic hinges in the beams are able to maintain their moment resisting capacities until the columns fail. The flexural ductility of an RC beam is dependent mainly on the failure mode, which in turn, is governed by the reinforcement details. In order to ensure a ductile mode of failure, it has been universally imposed as a basic requirement that all beam sections are under-reinforced. Maximum steel ratio below permissible by different codes plays a very important role to maintain good flexural ductility. For beams in seismic resistant structures, which are subjected to greater flexural ductility demands, more stringent requirements on the reinforcement detailing, such as the provision of confining reinforcement, are generally imposed.

It is generally considered that in the interests of safety, it is essential to provide a certain minimum level of flexural ductility and that for this purpose, just designing the beam sections to be under-reinforced is not sufficient. In most of the existing design codes, reinforcement detailing rules, which impose limits on either the tension steel ratio or the neutral axis depth, have been incorporated to guarantee the provision of minimum flexural ductility.

Very few flexural ductility experiments are available using Grade 500 steel and it is difficult to maintain sufficient ductility using high strength steel. The present experiment was designed, keeping above idea in mind, to provide detailed information on the sectional ductility properties (moment-curvature and ductility ratio) and neutral axis depth of rectangular beam using Grade 500 steel. The investigation involved physical testing of nine samples of rectangular beam produced considering three different Grade 500 steel ratios and concrete compressive strength. Sectional ductility mainly represented by the moment-curvature relationship of a section, and from this relation ductility ratio of a section section is determined. Detail test results from this study is presented in this paper.

RESEARCH SIGNIFICANCE

The problem of control on reinforcing steel becomes an important issue when one considers seismic loading especially when the structure is made of Grade 500 steel. In areas requiring design for seismic loading, ductility becomes an extremely

important consideration. The flexural ductility of the beam section may be evaluated in terms of a curvature ductility factor defined by energy absorption and dissipation of post elastic deformation for survival in major earthquakes. Thus, structures incapable of behaving in a ductile fashion must be designed for much higher seismic forces if collapse is to be avoided.

Generally, the ductility may be defined as the capacity of a material, section, structural element, or structure to undergo an excessive plastic deformation without a great loss of its resistance. In order to ensure enough ductility, all the structural elements should be correctly reinforced: the detailed rules created for that purpose, especially in codes of practice, should be respected. Besides, the ductility of the structural elements depends directly on the plastic rotation's capacity of the critical sections obtained through:

- The choice of suitable ductility characteristics of steel;
- The design of the section so that the position of the neutral axis in failure,d_a, is small; and
- The adoption of transversal reinforcement with spacings sufficiently small to guarantee a suitable confinement of the compressed concrete.

A convenient measure of the ductility of a section subjected to flexure or combined flexure and axial load is the ductility ratio μ of the ultimate curvature attainable without significant loss of strength, ϕ_u , to the curvature corresponding to first yield of the tension reinforcement, ϕ_y, as shown in following equation.

$$\mu = \frac{\phi_u}{\phi_y} \tag{1}$$

In performance-based design an adequate design is produced when a structure is dimensioned and detailed in such a way that the local deformation demands are smaller than their corresponding maximum tolerable limits for each performance level. Ideally, the deformation demands and deformation capacities must be checked at the critical region of all members (i.e., at all plastic hinges) by checking the maximum strain, the maximum strain ductility ratio [μ_ϵ], the maximum curvature, the maximum curvature ductility ratio, the maximum rotation or the maximum rotation ductility [μ_θ] with their corresponding limits.

This research would help to understand the ductility parameters discussed above. This would also provide information on role of concrete strength and Grade 500 steel ratio on moment-curvature relation, ductility ratio and neutral axis depth.

EXPERIMENTAL PROGRAM

Portland Composite Cement (PCC) conforming to BDS-EN 197 Part 1 was used for all mixes. Sylhet sand with specific gravity of 2.68 was used as fine aggregates. Crushed stone with specific gravity of 2.69 was used as coarse aggregates. Grade 500 steel was used as reinforcing steel.

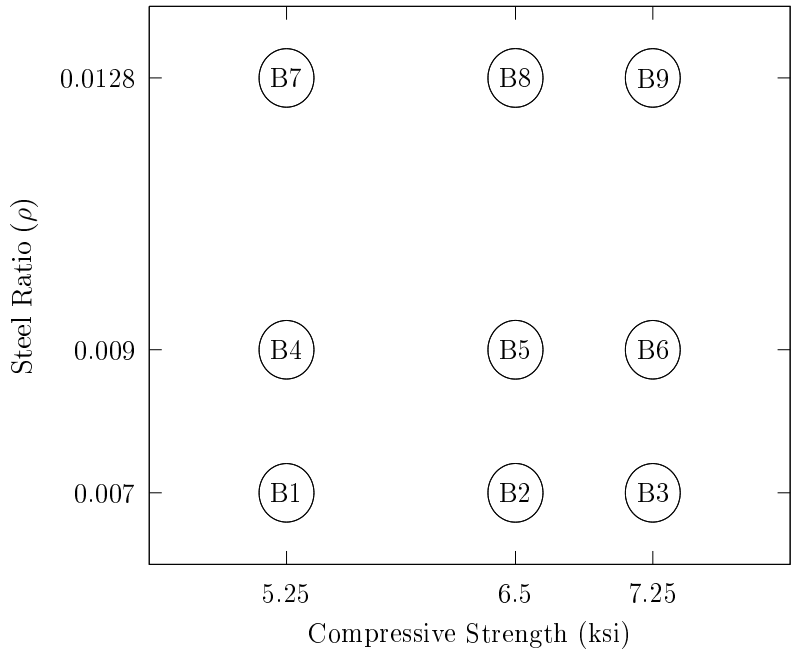

FIG. 1. Beam specimen in test frame

TABLE 1. Experimental parameters

Steel Ratio (ρ)	Compressive Strength ($f_c^{'}$, ksi)	Designation
0.007	5.25	B1
	6.5	B2
	7.25	B3
0.009	5.25	B4
	6.5	B5
	7.25	B6
0.0128	5.25	B7
	6.5	B8
	7.25	B9

Experimental design was prepared to understand the non-linear behavior of beam under monotonic loading for different steel ratios and concrete compressive compressive strengths. Three steel ratios and three concrete compressive strengths were taken, which is shown in Figure 1 and also given in Table 1.

The compressive strength of the concrete was determined by compression tests on typical samples of each mix of concrete. the type of mix design used to produce the concrete and the details of each mix are presented in Figure 2.

TABLE 2. Mix Design

Component	Mix design (kg/m^3)		
	5.0 ksi	6.0 ksi	7.0 ksi
Cement	435	480	520
Water	200	192	208
Sylhet Sand	710	730	668
Crushed Stone	1064	1094	1006
FA/TA	0.4	0.4	0.4
W/C	0.46	0.4	0.4
Density	2408	2412	2400
Achied Strength	5.25 ksi	6.5 ksi	7.25 ksi

Test Specimens

The beams were 7.5 feet long with a 10 in $\times$ 12 in cross section. They were simply supported and subjected to a symmetric loading composed of two equal concentrated forces. Such loading led, in theory, to pure bending between applied forces. The failure in the mentioned area between applied forces occurred always by simple bending. A total of nine rectangular concrete beams were fabricated and tested. Out of nine three beams were reinforced with 3 #6 Grade 500 steel rebars, another three beams were reinforced with 2#6 Grade 500 steel rebars and rest three beams were reinforced with 2#5 Grade 500 steel rebars in the tension side.

In order to assure a failure by flexure located between the point loads, a sufficient amount of stirrups was put in the zone outside the point loads in order to prevent failure by shear. The central zone between point loads had no stirrups to avoid confinement of the concrete. Since this zone was, in theory, in pure bending, the stirrups would not be necessary as far as the resistance is concerned. All beams were reinforced against shear failure by placing #3 Grade 500 steel at a spacing of 5 in centre to centre closed-type stirrups for 5.25 and 6.5 ksi concrete and 3 in centre to centre for 7.25 ksi concrete.

Loading Procedure

Concrete beams were simply supported and two point loading was applied. Monotonic loading was applied till the deflection of the beam stars to flow. The load was applied at 3 feet distance from the end of each beam. Load was applied in tons. Load was increasing by about 2 tons and cracking patterns were observed and recorded by camera. The experimental setup is shown in Figure 2. One linear voltage displacement transducers (LVDT) were placed at centre of the beam to measure the deflections at centre. The crack propagations were monitored using hand held microscope. Five holes were made in along the depth depth of the beam to measure the strain in the cross section. All strains, crack propagation and deflection measurements were measured at every load increment. The first crack load was noted immediately after the formation and all the cracks were

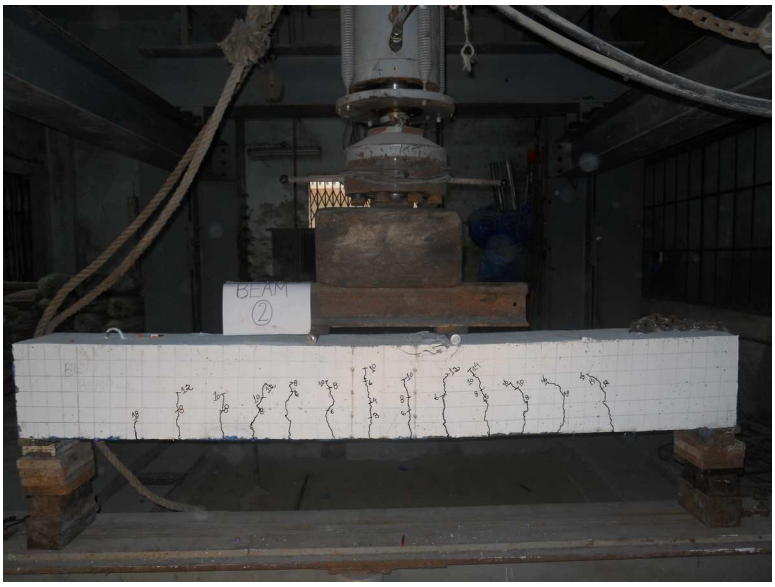

FIG. 2. Beam specimen in test frame

marked as and when they propagated in the beam. Propagation of cracks can be seen in the Figure 2.

TEST RESULTS

Strain

The tensile and compressive strains of reinforcement and concrete respectively were measured at every load increment. The strain measurements against the loads for B4, B8 and B9 beams are shown in Figure 3. The negative values show the compressive strains in the concrete, while the tensile strains in the reinforcement are shown in positive values.

The higher strains in B4 beam may be attributed to higher deflection due to low modulus of elasticity of beam. Beam B4 has lower steel ratio than other two beams shown here. The strains were linear in beams until yielding of steel and then rapidly increased before failure. The higher strains in concrete beams also show that good bond between steel and concrete existed till the yielding of steel. The strains, before final failure may have been higher than the strains mentioned here.

Neutral Axis Depth

As mentioned earlier, the necessary ductility may be achieved through an idealization of the section so that the position of the neutral axis in failure, defined by the parameter d_a, is limited to a certain maximum value. Such methodology is valid only for sections submitted to simple bending, such as the critical sections of the beams tested in this study. Therefore, the study of the evolution of the neutral axis' depth from the start to the failure load is very important. Also important is the value of the parameter d_a in failure and its relationship with the ductility

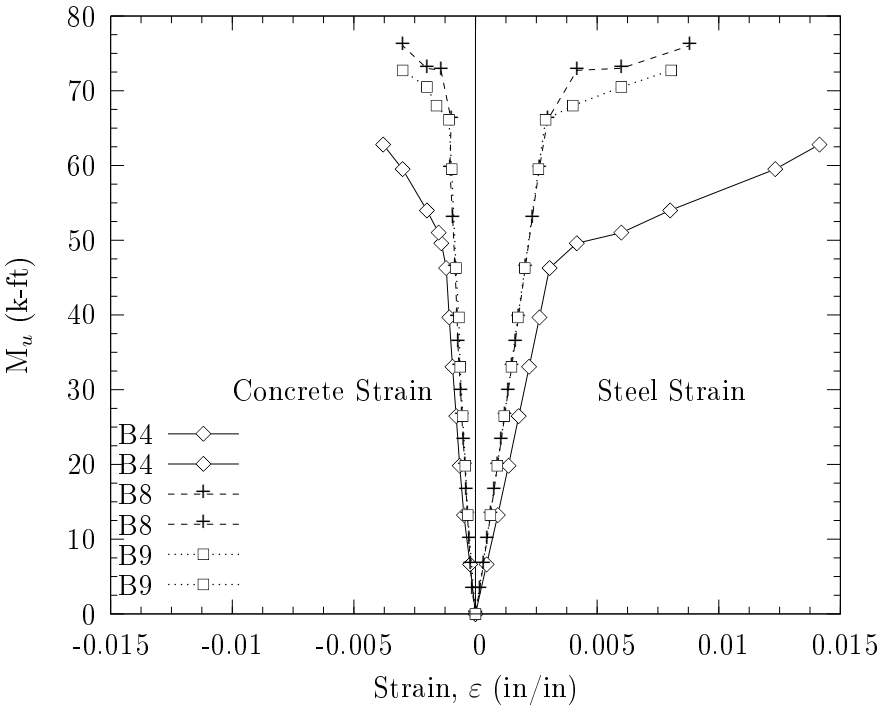

FIG. 3. Compressive and tensile strain in concrete and steel, respectively

itself. One of the objectives of this study is to check if these variations follow the same tendencies already observed and accepted for RC beam with normal strength steel. The experimental values of the position of the neutral axis at the critical section, for a given beam and for each load level, were simply calculated by intersecting the line obtained by regression analysis from the experimental strains along the height of the section with the vertical axes. The value of the bending moment at the midspan of each beam was statically calculated from the value of the total load applied to the beam at the considered load level. Figure 4 shows, for the critical section of the test beams, the evolution of the neutral axis' depth, taken throughout the tests up to failure. Such evolution is plotted according to the quotient M/M_u, M being the moment at the mid spans of the beams and where the failure has occurred is taken as M_u.

The analysis of the graph (Figure 4) shows the existence of three distinct zones of the behavior of the neutral axis' depth throughout the tests, which correspond to a typical evolution of the curves.

A first zone is identified by the rising of the neutral line as the load increases. It should be noted that the critical section is submitted to a positive moment, therefore, the rising of the neutral line corresponds to a decrease of d_a in the graph. In the uncracked state, the neutral axis is situated near the midheight of the section because of the influence of the reinforcement and it moves starting from this position. Generally, this phase is not clearly shown in the studied graphs, since the first crack observed in the critical section usually shows up at

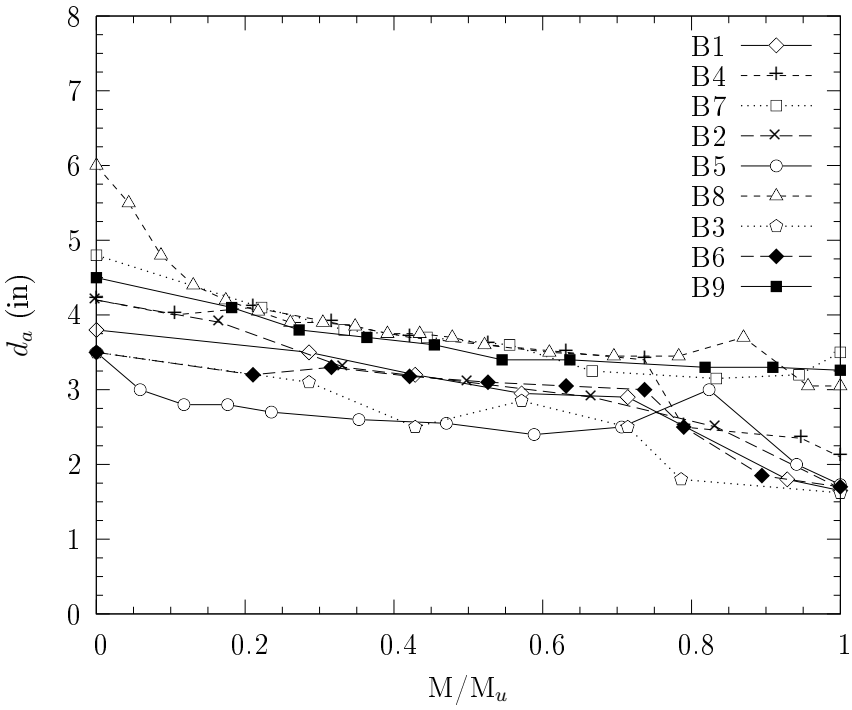

FIG. 4. Depth evolution of neutral axis with $\frac{M}{M_u}$

a low load level usually, 10-15% of the failure load. Therefore, at the first load stop for measurements, a crack had already taken place although it could not be spotted. The sudden variation of neutral axis' depth in the first points of the graphs confirms this fact. Thus, the first behavior zone corresponds to the development of a flexural crack, which increases in depth and width with the load.

The second zone corresponds to a stabilization of the neutral axis' depth as the beam suffers considerable deformations while the load increases slowly. This behavior is due to the stabilization of the crack, and corresponds to a loading interval where the main crack does not develop any further. In fact, more cracks appear in the central zone of the beams.

Finally, the third behavior zone generally corresponds to an abrupt rise of the neutral axis up to the ultimate moment of the critical section. This behavior starts with the yielding of the longitudinal tensile reinforcement, forcing the main crack to develop even further due to the sudden rise of the reinforcement strains up to the section failure.

The method of limiting the neutral axis depth in order to ensure provision of minimum flexural ductility has been adopted by a number of design codes. However, different design codes set maximum limits to the neutral axis depth in different ways. For instance, the design code NZS 3101 limits the neutral axis depth to not more than a certain fraction of the neutral axis depth of the balanced section, while the design codes BS 8110, EC 2 and GBJ 11 limit the neutral axis

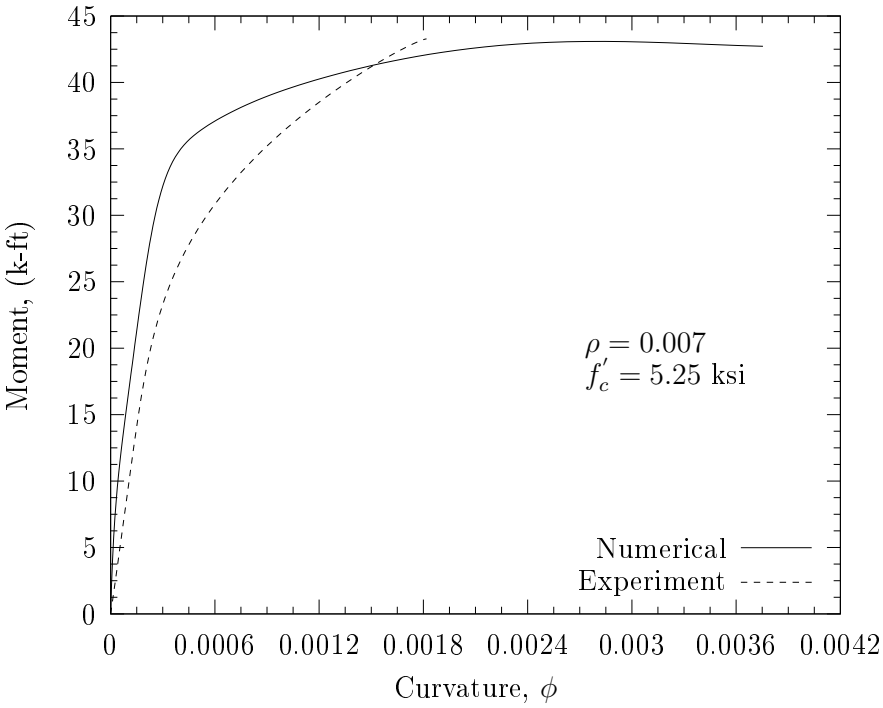

FIG. 5. Comparison of experimental and numerical moment-curvature for $f_c^{'} = 5.25$ **ksi**

depth to not more than a certain fraction of the effective depth. The maximum limits set to the neutral axis depth in these codes are applicable to both the case of singly reinforced sections with no compression reinforcement added and the case of doubly reinforced sections with compression reinforcement added.

Moment Curvature Curves

Moment-curvature curves of the beam sections experimented are shown in Figure 5 to Figure 13. It can be seen that the moment-curvature curves are almost linear before the peak moment is reached and there is a fairly long yield plateau at the post-peak stage. As the experiments were load control post yield plateau decrease of plastic moment could not be replicated. From moment-curvature relation information about fleuxural strength, flexural stiffness and more importantly flexural ductility can be extracted.

Numerical moment-curvatures were calculated for the same cross section for all nine beams. These are compared with experimental moment curvature results and shown in Figure 5 to Figure 7. Numerical results matched well with experimental result. This proves the robustness of the theory of calculating moment-curvature relation for cross section. Thus, numerical results may be used for further analysis as conducting experiment is always not feasible and costly too.

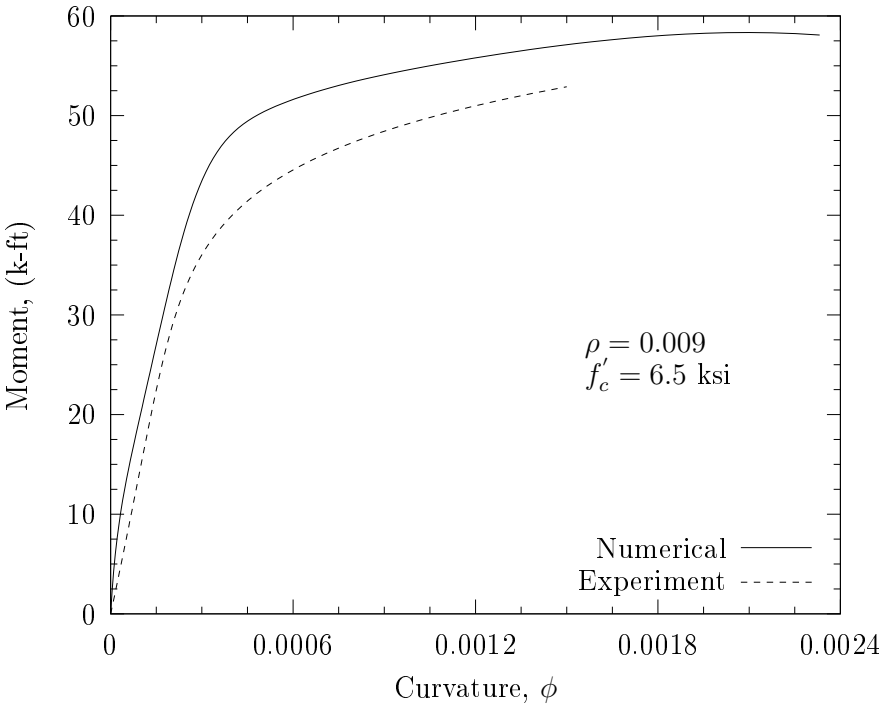

FIG. 6. Comparison of experimental and numerical moment-curvature for $f_c^{'} = 5.25$ **ksi**

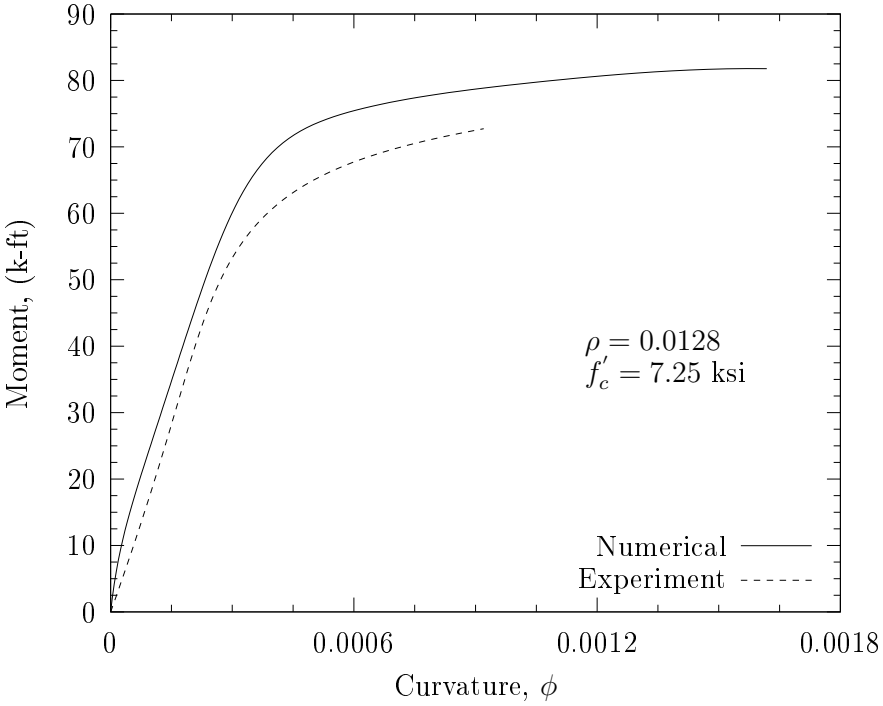

FIG. 7. Comparison of experimental and numerical moment-curvature for $f_c^{'} = 5.25$ **ksi**

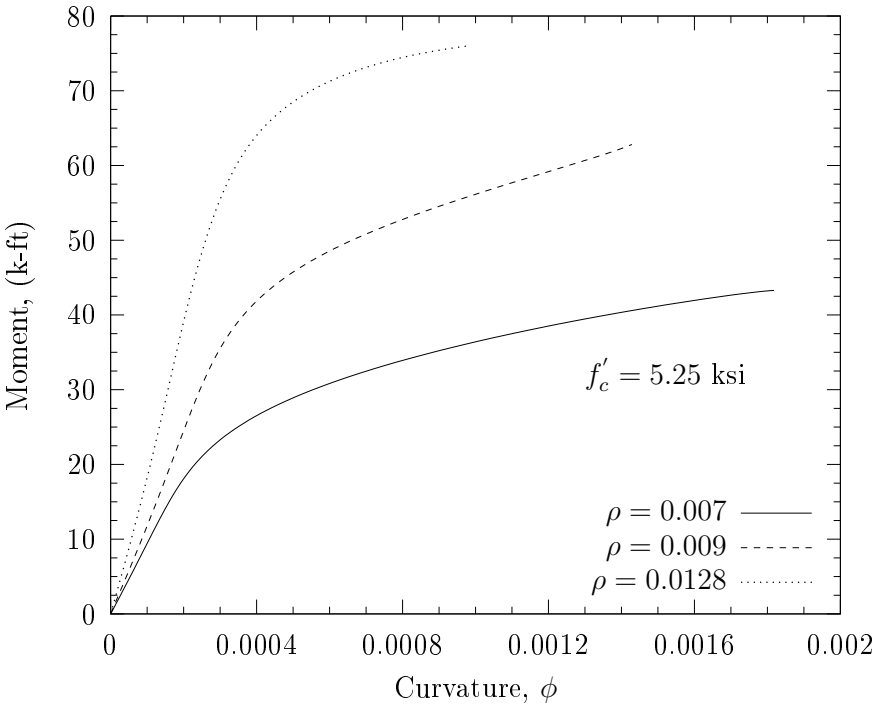

FIG. 8. Moment-curvature relations for $f_c' = 5.25$ ksi

Role of Steel Ratio

Figure 8 to Figure 10 show the role of steel ratio on moment-curvature relations. It can be seen from these figures that both flexure strenght and stiffness is increased with the increase of steel ratio. It can also be observed from these figures that low steel ratio gives more ductility than high steel ratio. In all cases the steel ratio is below the balanced steel ratio for that respective cross section. In ductility based design it is very important to keep the steel ratio low. It is true that high strength steel produces lower ductility than low strength steel. However, this loss of ductility can be compensated using lower steel ratio. High strength steel gives lower steel area for a particular Moment and cross section per se, which in turn ensure low steel ratio.

Role of Concrete Compressive Strength

Figure 11 to Figure 13 show the role of concrete compressive strength on moment-curvature relations. It can be seen from these figures that no significant effect of compressive strength of concrete on moment-curvature relationships were observed. Though numerical results show otherwise. This may be due to the fact that the strain controlled experiments could not be performed. Complete moment-curvature curve up to failure could not be traced. From ductility ratio some idea of concrete compressive strength is observed. It can be concluded that no significant change has been observed in both flexural strength and stiffness as concrete compressive strength chages.

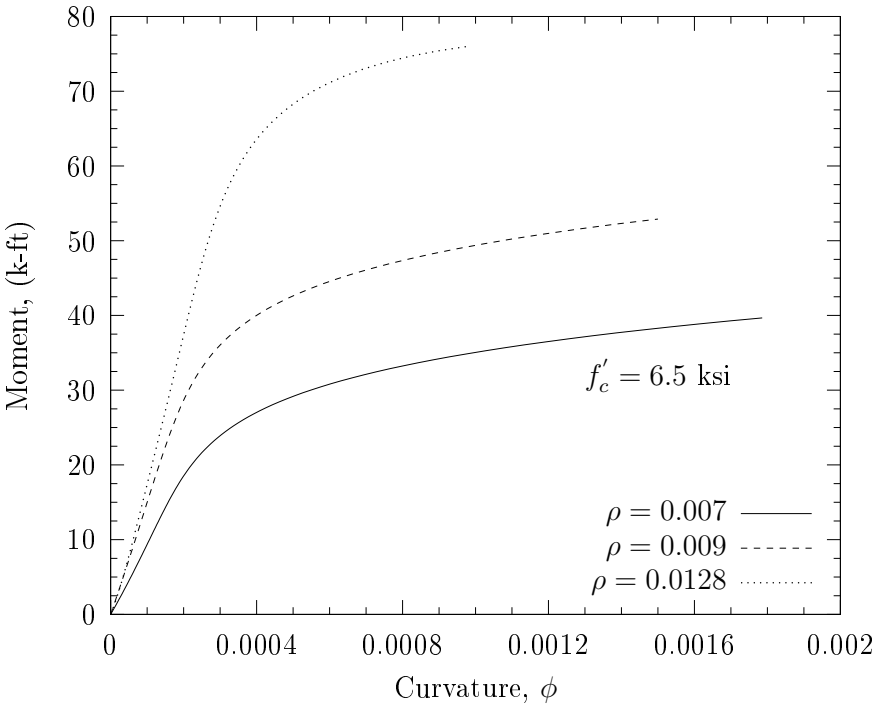

FIG. 9. Moment-curvature relations for $f_c' = 6.5$ ksi

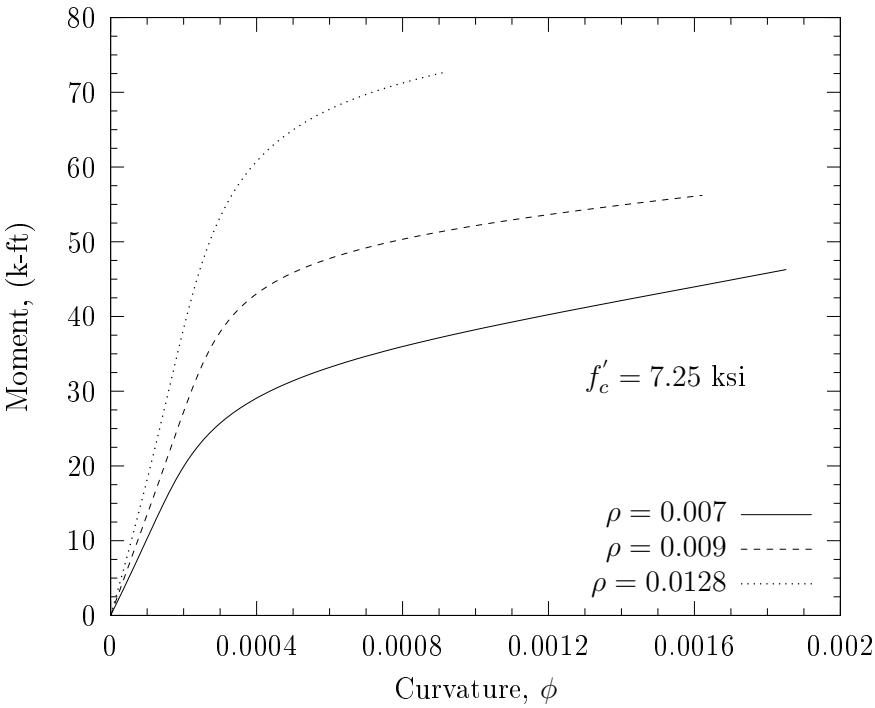

FIG. 10. Moment-curvature relations for $f_c' = 7.25$ ksi

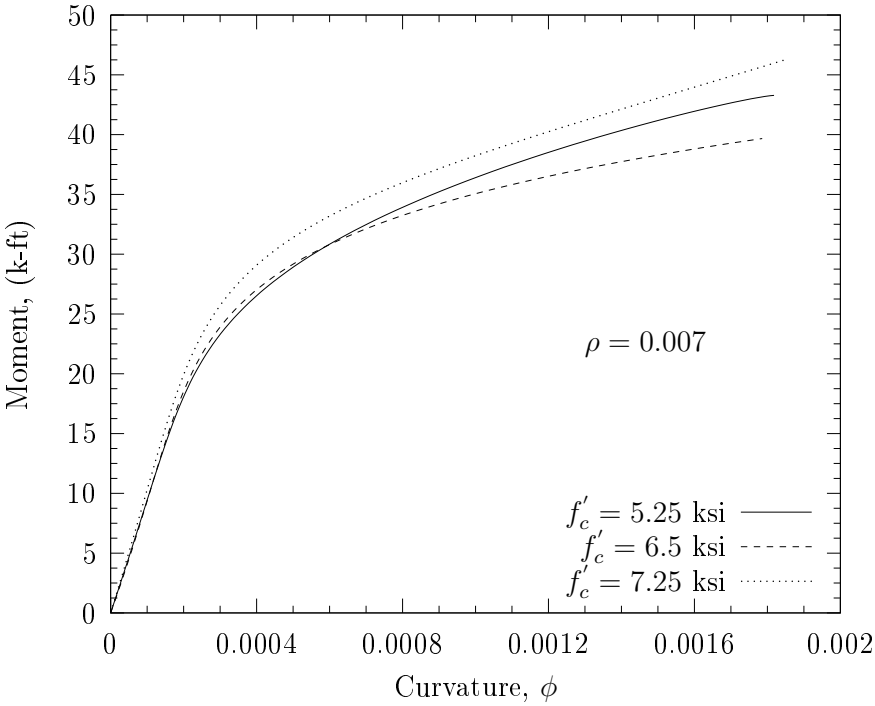

FIG. 11. Moment-curvature relations for $\rho = 0.007$

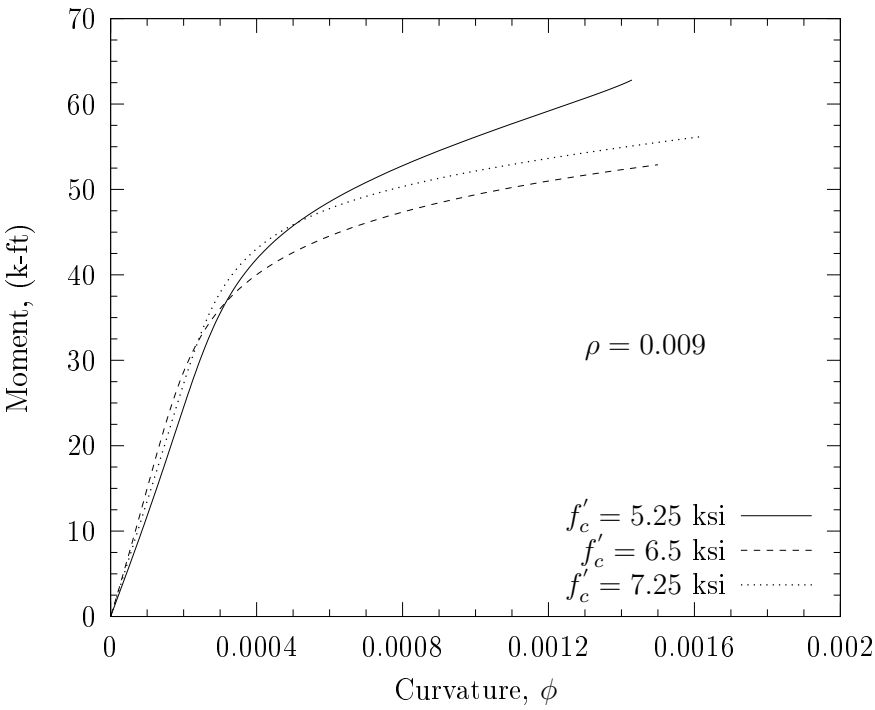

FIG. 12. Moment-curvature relations for $\rho = 0.009$

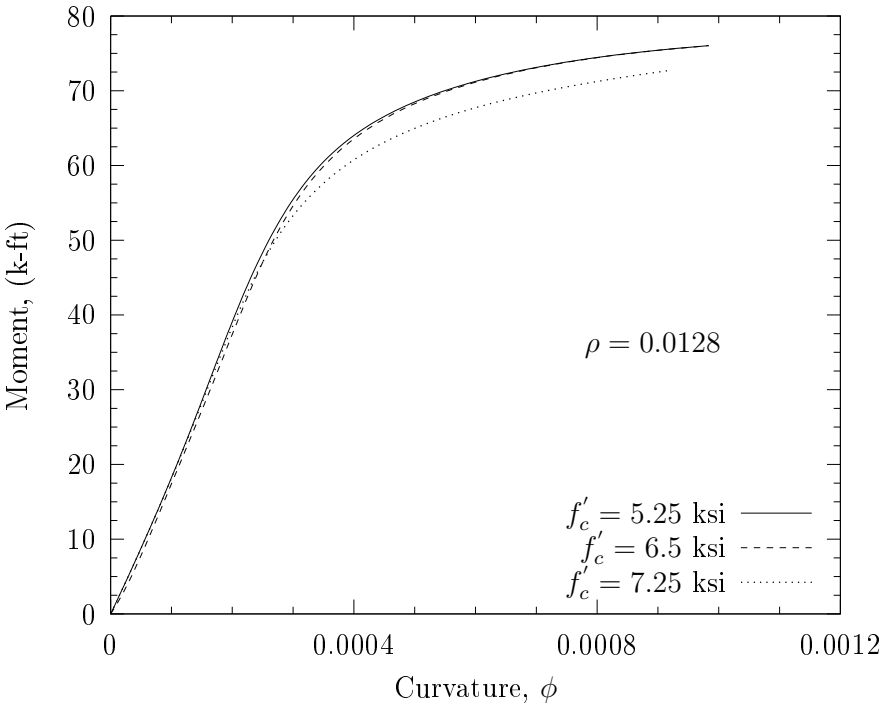

FIG. 13. Moment-curvature relations for $\rho = 0.0128$

Ductility Ratio

Figure 14 shows the relationship of ductility ratio with concrete compressive strength for different steel ratio. It can seen from the figure that no significant increase of ductility ratio is observed with concrete compressive strength. However, lower steel ratio gives higer ductility ratio. It is recommended from ductility based design that there must be a upper limit of steel ratio apart from ρ_{max} provided in different codes from ductility point of view.

CONCLUSIONS

The advantages and disadvantages of using higher strength materials are now clear. The use of a higher strength steel would allow a higher flexural strength and stiffnes to be achieved while maintaining the same minimum level of flexural ductility if steel ratio is properly selected. On the other hand, the use of a higher strength concrete would not allow a higher flexural strength and stiffness to be achieved while maintaining the same minimum level of flexural ductility; it only allows the use of a smaller steel area for a given flexural strength requirement to save the amount of steel needed and to avoid steel congestion.

Proper bond between high strength concrete and high strength steel is observed even after post yield period. Strain curve and moment-curvature curve both validate the compatibility between the materials.

From the tests, the evolution of the position of the neutral axis for high strength beams as the load increases, is identical to that reported for RC concrete beams with normal strength steel. The behavior of the formation and the growth

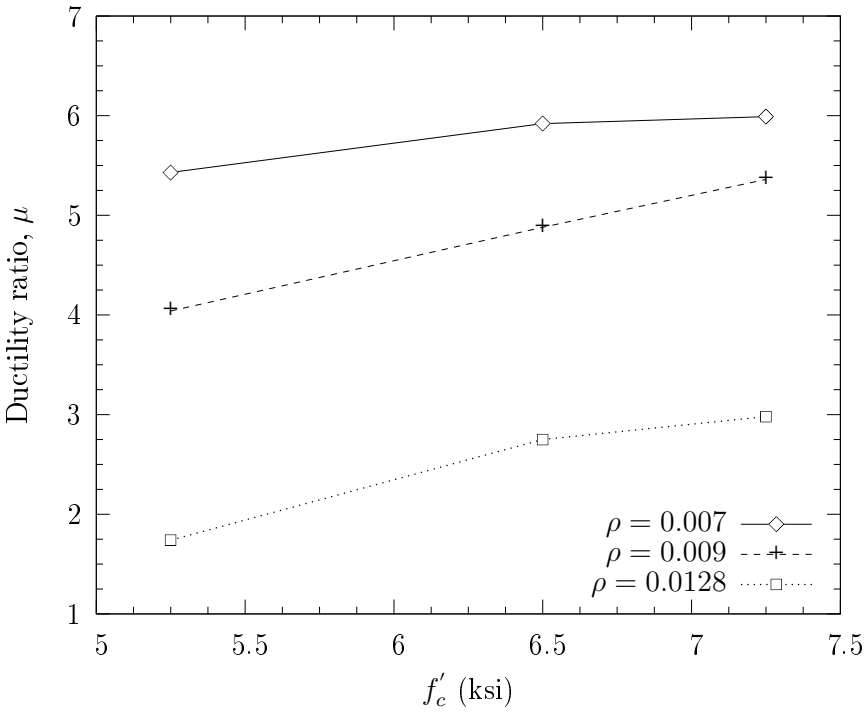

FIG. 14. Variation of ductility ratio

of the cracks for normal-strength steel beams seem to be also valid for concrete beams using high-strength steel.

There must be upper limit of steel ratio apart from ρ_{max} provided in codes of practice from ductility ratio point of view.

ACKNOWLEDGMENT

This undergraduate research project, conducted using BUET laboratory and by BUET Level 4 Term II students (Shohana Iffat and Kazi Maina), is funded by BSRM and HOLCIM.